Appendix C

Quasi 1-D analysis of a circular, compressible, turbulent jet laden with water droplets

September 27, 2001

Abstract

Recent experimental studies indicate that presence of small amount of liquid droplets reduces the Overall Sound Pressure Level (OASPL) of a jet. Present study is aimed at numerically investigating the effect of liquid particles on the overall flow quantities of a heated, compressible round jet. The jet is assumed perfectly expanded. A quasi-1D model was developed for this purpose which uses area-averaged quantities that satisfy integral conservation equations. Special attention is given to represent the early development region since it is acoustically important. Approximate velocity and temperature profiles were assumed in this region to evaluate entrainment rate. Experimental correlations were used to obtain spreading rate of shear layer. The base flow thus obtained is then laden with water droplets at the exit of the nozzle. Mass, momentum and energy coupling between the two phases is represented using empirical relations. Droplet size and mass loading are varied to observe their effect on flow variables.

Nomenclature

ρ_g: Bulk mean density of gas phase $[kg/m^3]$
u_g: Bulk mean velocity of gas phase $[m/s]$
m_p: Mass of one particle [kg]
m_e: Entrained mass per unit length in streamwise direction [kg/m-s]
P: Pressure [Pa]
T_g: Bulk mean temperature of the gas phase [K]
T_p: Temperature of liquid particles [K]
D: Nozzle diameter [m]
u_p: Particle velocity [m/s]
n: Particle flux through any cross section of the jet $[s^{-1}]$
A: Effective area of the jet $[m^2]$
C_{pg}: Specific heat at constant pressure of the gaseous phase [J/kg-K]
L: Latent heat of vaporization of water [J/kg]
Cp: Specific heat of liquid water [J/kg-K]
R: Gas constant per unit mass [J/kg-K]
h: Convective heat transfer coefficient $[J/m^2sK]$
h_D: Mass diffusivity $[kg/m^2s]$
D_m: Diffusion constant $[m^2/s]$
C_2: Non-dimensional entrainment rate
C_D: Drag coefficient
α: Entrainment coefficient

M_c: Convective Mach number
a: Radius of droplet [m];
Speed of sound [m/s]
δ_{99}: 99% velocity thickness [m]
$\delta_{1/2}$: 1/2 velocity thickness [m]
δ_{ω}: Vorticity thickness [m]
δ_{vis}: Visual thickness [m]
δ_{pit}: Pitot tube thickness [m]
M: Momentum flux $[kg - m/s^2]$
m: Mass flux [kg/s]
r: Radial distance from jet centerline [m]
Re: Reynolds number
Pr: Prandtl number
Sc: Schmidt number
Bi: Biot number
Sh: Sherwood number
Nu: Nusselt number

Subscripts

g: Gaseous phase
p: Particle
e: Entrainment
w: Liquid water
v: Water vapor
a, air: Air
sat: Saturated
0: Jet exit
c: Centerline
∞: Ambient

1 Introduction

Supersonic jet noise can be classified into three distinct components- shock associated noise, screech tones, and turbulent mixing noise (Krothapalli and Washington, 1998). The turbulent mixing noise is the most dominant contributor to the OASPL. A novel approach to jet noise reduction is to use water injection to minimize the turbulent mixing noise. The goal here is to use minimal mass loading of the gas phase with water (less than 10%) to achieve substantial reduction in OASPL. Higher mass loading is impractical as the aircraft has to carry the water to be injected into the jet.

A 1-D model of the jet was developed. It uses continuity, momentum and energy equations to march variables in the streamwise direction. Area-integrated form of the conservation equations are used. Variables considered are area-averaged flow variables. The assumption that these equations represent the actual system to a fairly good accuracy can be justified by the following analysis.

1.1 Integral form of RANS equations

Since algebra can grow quite tedious with cylindrical coordinates, we will consider a plane jet for illustration purpose. Also, to simplify the analysis, we assume incompressible flow. First, consider continuity equation for turbulent flow.

$$\frac{\partial \overline{u}}{\partial x} + \frac{\partial \overline{v}}{\partial y} = 0$$

Integrating over y,

$$\frac{\partial}{\partial x}\left(\int_0^H \overline{u} dy\right) + \overline{v}|_0^H = 0$$

$$\frac{\partial}{\partial x}\left(\int_0^H \overline{u} dy\right) = -(\overline{v}|_H - \overline{v}|_0)$$

but $\overline{v}|_H = \frac{-m_e}{\rho}$ *and* $\overline{v}|_0 = 0$ by symmetry.
hence,

$$\frac{d}{dx}\left(\int_0^H \overline{u} dy\right) = \frac{m_e}{\rho} \tag{1}$$

Now consider the x-momentum equation in conservative form-

$$\frac{\partial \overline{u}^2}{\partial x} + \frac{\partial \overline{uv}}{\partial y} + \frac{\partial}{\partial x}\left(\overline{u'^2}\right) + \frac{\partial}{\partial y}\left(\overline{u'v'}\right) = -\frac{1}{\rho}\frac{\partial \overline{P}}{\partial x} + \nu\left(\frac{\partial^2 \overline{u}}{\partial x^2} + \frac{\partial^2 \overline{u}}{\partial y^2}\right)$$

Integrating over area perpendicular to the x-axis,

$$\frac{d}{dx}\left(\int_0^H \overline{u}^2 dy\right) + \left(\overline{uv}\right)\Big|_0^H + \frac{d}{dx}\left(\int_0^H \frac{\overline{u'^2}}{2} dy\right) + \left(\overline{u'v'}\right)\Big|_0^H = -\int_0^H \frac{1}{\rho_o}\frac{\partial \overline{P}}{\partial x} dy + \nu\frac{\partial^2}{\partial x^2}\left(\int_0^H \overline{u} dy\right) + \nu\frac{\partial \overline{u}}{\partial y}\Big|_0^H$$

Last term on each side, and the second term on the LHS are zero, when evaluated at y=0, H. Since mean pressure is assumed to be constant everywhere, $\partial \overline{P}/\partial x = 0$. Also, for a turbulent jet, viscous stresses are unimportant. So, simplified form of the above equation becomes:

$$\frac{d}{dx}\left[\int_0^H \left(\overline{u}^2 + \frac{\overline{u'^2}}{2}\right) dy\right] \approx 0$$

We know that u' is less than roughly 10% of $\overline{u}$ in magnitude. Hence second term in the bracket is even smaller than the first term. The above equation is then approximately equivalent to

$$\frac{d}{dx}\left(\int_0^H \overline{u}^2 dy\right) = 0 \tag{2}$$

This is the integral form of the momentum equation. Energy equation can also be treated similarly. We will apply these equations to the present case of compressible jet using mean variables. In order to completely specify the problem, one needs to specify the entrainment mass rate distribution. To obtain this, experimental data about spreading rates of jet and its shear layer are used. Such data is presented by Papamoschou and Murakami (2000), Lele and Freund (2001) and Dimotakis *et al* (2000). Experiments related to prediction of entrainment rate were done by Hill (1972), and Ricou and Spalding (1961). Relation between different measures of spreading rates, namely, vorticity thichness, visual thickness and pitot tube thichness was obtained from Papamoschou and Roshko (1988). Experimental and analytical study of jet entrainment is also found due to Zaman (1998). Further, DNS study of particle-laden mixing layer by Miller and Bellan (1999) was found to be a useful reference for phase coupling relations.

2 Problem formulation and governing equations

A circular jet issuing into quiescent atmosphere is considered. The geometry and jet exit conditions were those used in the experiments by Krothapalli and Washington (1998). Jet diameter is 29 mm. The jet is assumed to be perfectly expanded i.e., pressure everywhere outside the nozzle is equal to atmospheric pressure and the nozzle is operating under design conditions. The jet Mach number is varied as a parameter. Mach number at the exit determines the exit and stagnation conditions through the requirements of isentropy. Jet Mach number was kept 1.44 in this study. Stagnation temperature was set to 600 K. Liquid water was introduced in the form of tiny spherical droplets at the jet exit at ambient temperature. Ambient temperature was taken as 298 K. Initial velocity of the droplets at exit was 50 m/s. "n" number of water droplets of instantaneous mass m_p cross any given cross section of the jet per unit time. We can extend our analysis to accomodate different droplet sizes and corresponding number densities.

As discussed earlier, approximate integral equations will be used for marching. These 1-D equations with the streamwise coordinate x as the independent variable are written in control volume form. Entrainment rate is calculated simultaneously (discussed in detail later), and the equations are spatially marched. But before doing that, we define the equivalent plug profiles for velocity, density and temperature and equivalent area of the jet in such a way that these quantities confirm to the conservation equations and constitutive relation. These variables are then used as dependent variables which are solved for. Definition of such variables is illustrated in figure (1) below.

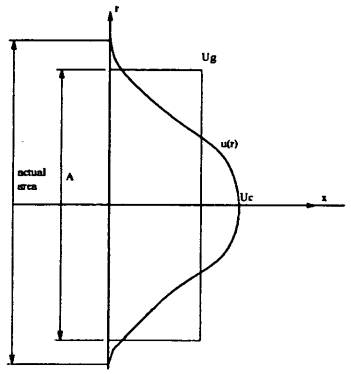

Figure 1: Defining area averaged variables

Continuity equation:

$$nm_p\Big|_x + (\rho_g A u_g)\Big|_x + m_e\Big|_x \Delta x = (\rho_g A u_g)\Big|_{x+\Delta x} + nm_p\Big|_{x+\Delta x}$$

$$\frac{d}{dx}(\rho_g A u_g) + \frac{d}{dx}(nm_p) = m_e \tag{3}$$

Momentum balance:

Momentum in + Force in the +ve x direction = Momentum out

$$(\rho_g u_g^2 A)\Big|_x + (nm_p u_p)\Big|_x = (\rho_g u_g^2 A)\Big|_{x+\Delta x} + (nm_p u_p)\Big|_{x+\Delta x}$$

Net pressure force is zero because pressure is constant everywhere (atmospheric) and the control volume is closed. Above equation then becomes, in differential form,

$$\frac{d}{dx}(\rho_g A u_g^2) + \frac{d}{dx}(n m_p u_p) = 0 \tag{4}$$

Energy balance:

$$(Thermal + KineticEnergy)\Big|_{in} = (Thermal + KineticEnergy)\Big|_{out}$$

$$(\rho_g u_g A C_{pg} T_g)\Big|_x + (n m_p C_p T_p)\Big|_x + (\tfrac{1}{2}\rho_g u_g^3 A)\Big|_x + (n m_p \tfrac{u_p^2}{2})\Big|x + m_e C_{p,air} T_{amb} \Delta x$$
$$= (\rho_g u_g A C_{pg} T_g)\Big|_{x+\Delta x} + (n m_p C_p T_p)\Big|_{x+\Delta x} + (\tfrac{1}{2}\rho_g u_g^3 A)\Big|_{x+\Delta x} + (n m_p \tfrac{u_p^2}{2})\Big|_{x+\Delta x}$$

$$\frac{d}{dx}(\rho_g u_g A C_{pg} T_g) + \frac{d}{dx}(n m_p C_p T_p) + \frac{d}{dx}(\frac{1}{2}\rho_g u_g^3 A) + \frac{d}{dx}(n m_p \frac{u_p^2}{2}) = m_e C_{p,air} T_{amb} \tag{5}$$

In addition to these conservation equations, we also have relations describing the coupling between the two phases corresponding to mass, momentum and heat transfer. Rate of mass transfer between a water droplet and the surrounding gas is determined by the difference between concentrations of water vapor at the surface and away from the surface. It is governed by the relation:

$$\begin{aligned}
\tfrac{dm_p}{dt} &= -(Area) h_D ln(1 + B_m) \\
\tfrac{dm_p}{dx} u_p &= -4\pi a^2 h_D ln(1 + B_m) \\
\tfrac{dm_p}{dx} &= -\tfrac{-4\pi a^2}{u_p} h_D ln(1 + B_m)
\end{aligned} \tag{6}$$

where $B_m = \frac{X_{sat} - X_v}{1 - X_{sat}}$, X_{sat} and X_v being mass fractions of vapor under saturated and actual conditions respectively. h_D is mass diffusivity of water vapor in air in $kg/m^2 s$.

X_{sat} and X_v are calculated as follows:

If m_v is the mass flux of water vapor through any cross section of the jet, then

$$\rho_v = \frac{m_v \Delta t}{A u_g \Delta t} = \frac{m_v}{A u_g}$$

Since water vapor is generated only due to evaporation of droplets,

$$m_v = n(m_{po} - m_p)$$

Water vapor density under saturated conditions is

$$\rho_{sat} = \frac{P_{sat}}{R_v T_g}$$

with R_v being the gas constant for water vapor and P_{sat} the saturation pressure given by (Miller and Bellan, 1999)

$$P_{sat} = P_{atm} exp\left\{ \frac{L}{R_v}\left(\frac{1}{T_B} - \frac{1}{T_p}\right)\right\}$$

Here T_B is the boiling temperature of water at atmospheric pressure, L is the latent heat of vaporization of water (assumed constant), and T_p is particle temperature. Now, patial pressure of dry air under saturated condition is $P_{a,sat} = P_{atm} - P_{sat}$. So, the density of dry air in saturated air becomes

$$\rho_{a,sat} = \frac{P_{a,sat}}{R_{air}T_g}$$

Then, the total density of gaseous phase will be

$$\rho_{tot,sat} = \rho_{a,sat} + \rho_{sat}$$

The mass fractions now become

$$X_{sat} = \frac{\rho_{sat}}{\rho_{tot,sat}} \quad and \quad X_v = \frac{\rho_v}{\rho_{gas}}$$

Mass diffusivity is given by

$$h_D = Sh \quad \rho_g \frac{D_m}{(2a)}$$

Where
Sh = Sherwood number
D_m=Diffusivity of water vapor in air = $2.93 \times 10^{-5} m^2/s$
2a=Length scale (droplet diameter)

Sherwood number is dependent on Reynolds number based on the empirical relation

$$Sh = 2 + 0.552 Sc^{1/3} Re^{1/2} \tag{8}$$

Here, Sc is Schmidt number and its value is 0.608 for water vapor in air. Reynolds number is defined based on the particle diameter and slip velocity.

$$Re = \frac{\rho_g |u_g - u_p|(2a)}{\mu_g} \tag{9}$$

Momentum coupling relation is based on experimentally measured values of drag coefficient, C_D, for a range of Reynolds number. Drag force is

$$F_D = C_D \frac{1}{2} \rho_g (u_g - u_p)^2 (\pi a^2) \tag{10}$$

But $F_D = m_p du_p/dt = m_p u_p du_p/dx$. Hence,

$$\frac{du_p}{dx} = \frac{1}{m_p u_p} C_D \frac{1}{2} \rho_g (u_g - u_p)^2 (\pi a^2) sign(u_g - u_p) \tag{11}$$

Variation of C_D with Re used here is shown below (Donley, 1991).

Heat transfer between the two phases is governed by the temperature difference between the particle surface and the surrounding fluid through the relation

$$h(T_p - T_g) 4\pi a^2 = \frac{\Delta m_p}{\Delta t} [L + C_p (T_{evap} - T_p)] - m_p C_p \frac{\Delta T_p}{\Delta t}$$

Substituting $\Delta t = \Delta x/u_p$,

$$h(T_p - T_g) \frac{4\pi a^2}{u_p} = \frac{dm_p}{dx} [L + C_p (T_{evap} - T_p)] - m_p C_p \frac{dT_p}{dx} \tag{12}$$

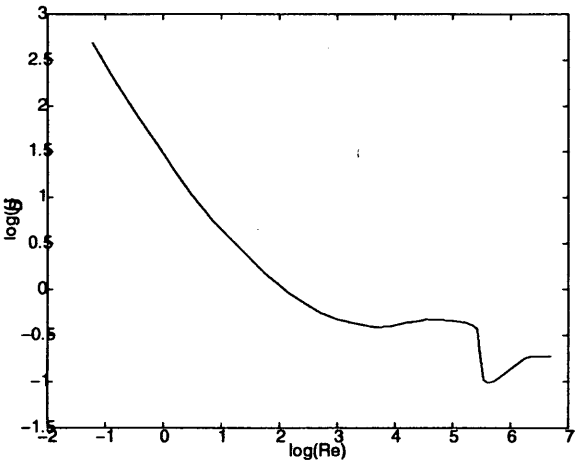

Figure 2: Variation of drag coefficient with Reynolds number

Where L is the latent heat of vaporization of water. Its value is $2.5 \times 10^6 J/kg$. Here it is assumed that the temperature inside a droplet is approximately constant i.e. temperature gradients inside a particle are small. This is justified when particle size is small and its conductivity is high. A plot of particle Biot number evolution (Fig. (3)) for the particle size of 26 microns shows that $Bi = hd/6k_w < 0.1$ and above assumption is valid.

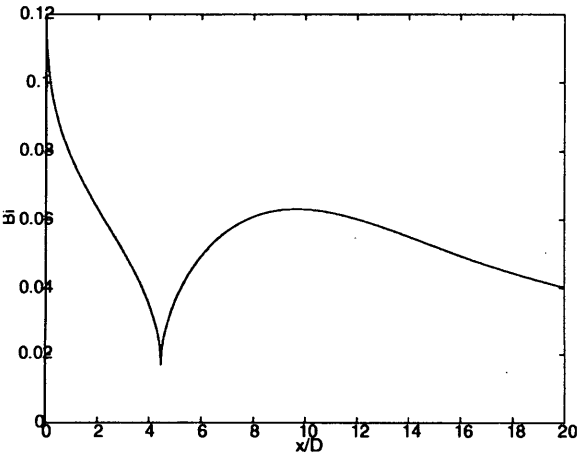

Figure 3: Evolution of Biot number

To compute convective heat transfer coefficient we use the following relation

$$Nu = 2 + 0.552 Pr^{1/3} Re^{1/2} \tag{13}$$

Now, changes in thermodynamic properties of the gaseous mixture are functions of its composition i.e. fraction of water vapor present. Variations in these properties are governed by the requirement that, in an adiabatic mixing process, total energy is conserved. We define the bulk properties of the gas phase in such a way that these properties, when used to obtain energy,

give the same total energy as the sum of the energies of the individual gaseous components, assuming a hypothetical adiabatic mixing process.

Applying the above statement to the control volume,

$$(\rho_g u_g A C_{pg})\Big|_{x+\Delta x} T\Big|_{x+\Delta x} = (\rho_g u_g A C_{pg})\Big|_x T\Big|_{x+\Delta x} + m_e \Big|_x \Delta x C_{p,air} T\Big|_{x+\Delta x} + n\frac{dm_p}{dx} C_{p,v} T\Big|_{x+\Delta x}$$

$$\frac{d}{dx}(\rho_g u_g A C_{pg}) = m_e C_{p,air} + n\frac{dm_p}{dx} C_{p,v} \tag{14}$$

Same equation can also be obtained by mass-averaging the component Cp values.
It should be noted that partial pressures of gases add to produce total pressure.

$$P = P_a + P_v$$

$$P = (\rho_a R_a + \rho_v R_v) T_g \tag{15}$$

Also, densities add.

$$\rho_g = \rho_a + \rho_v \tag{16}$$

Thus, we have a set of the above equations and the following unknowns: $u_g, \rho_g, T_g, C_{pg}, u_p, m_p, T_p, A$.

3 Solution procedure

Solution was marched streamwise using Euler explicit method. This required derivatives of some of the dependent variables at every step. It was observed that this produces an ill-conditioned system of equations that tends to diverge. As a remedy, this system was diagonalized by defining two more variables related to the gaseous phase, namely, mass flow rate and enthalpy of the gas.

$$m_g = \rho_g u_g A$$

$$\mathrm{h}_g = C_{pg} T_g$$

Henceforth, we adopt a notation in which a dot (.) above a variable indicates derivative with respect to x. Variables pertaining to particles, u_p, T_p, m_p can be easily decoupled using the coupling relations in the following way:

Equation (6),(11) ,(12) respectively give:

$$\dot{m_p} = -\frac{4\pi a^2}{u_p} h_D ln(1 + B_m) \tag{17}$$

$$\dot{u_p} = \frac{1}{m_p u_p} C_D \tfrac{1}{2} \rho_g (u_g - u_p)^2 \pi a^2 sign(u_g - u_p) \tag{18}$$

$$\dot{T_p} = \frac{1}{m_p C_p} \left\{ h(T_p - T_g)\frac{4\pi a^2}{u_p} - \dot{m_p}[L + C_p(T_{evap} - T_p)] \right\} \tag{19}$$

Variables corresponding to the gas phase are then decoupled as follows:
Equation (3) gives:

$$\dot{m_g} = m_e - n\dot{m_p} \tag{20}$$

Equation (4) is:

$$\frac{d}{dx}(m_g u_g) + \frac{d}{dx}(n m_p u_p) = 0$$
$$m_g \dot{u_g} + u_g \dot{m_g} + n(\dot{m_p} u_p + \dot{u_p} m_p) = 0$$
$$m_g \dot{u_g} = -u_g \dot{m_g} - n(\dot{m_p} u_p + \dot{u_p} m_p)$$

Using eq.(20), we get

$$m_g \dot{u_g} = -u_g m_e + n u_g \dot{m_p} - n \dot{m_p} u_p - n \dot{u_p} m_p$$
$$m_g \dot{u_g} = -u_g m_e + n(u_g - u_p)\dot{m_p} - n \dot{u_p} m_p$$
$$\dot{u_g} = \frac{1}{m_g}[-u_g m_e + n(u_g - u_p)\dot{m_p} - n \dot{u_p} m_p] \tag{21}$$

Energy balance equation was:

$$\frac{d}{dx}(m_g h_g) + \frac{d}{dx}(n m_p C_p T_p) + \frac{d}{dx}(\frac{1}{2} m_g u_g^2) + \frac{d}{dx}(n m_p \frac{u_p^2}{2}) = m_e h_e$$

Where $h_e = C_{p,air} T_{amb}$
Rearranging,

$$\dot{h_g} = \frac{1}{m_g}\{m_e h_e - \dot{m_g} h_g - \frac{1}{2}\dot{m_g} u_g^2 - m_g u_g \dot{u_g} - n[\dot{m_p}(C_p T_p + \frac{1}{2} u_p^2) + m_p C_p \dot{T_p} + m_p u_p \dot{u_p}]\} \tag{22}$$

Equation (14) was:

$$\frac{d}{dx}(\rho_g u_g A C_{pg}) = m_e C_{p,air} + n \frac{dm_p}{dx} C_{p,v}$$

This gives:

$$m_g \dot{C_{p,g}} = m_e C_{p,air} + n \dot{m_p} C_{p,v} - \dot{m_g} C_{p,g} \tag{23}$$

Equations (17) to (23) form a diagonal system of linear algebraic equations in $u_p, T_p, m_p, u_g, m_g, h_g, C_{pg}$. After advancing every time step, all other variables are updated as:

$$T_g = h_g / C_{p,g}$$
$$\rho_g = \rho_a + \rho_v \tag{24}$$

Where $\rho_a = \frac{\dot{m}_{air}}{A u_g}$ and $\rho_v = \frac{\dot{m}_{vapor}}{A u_g}$

$$\dot{m}_{air} = m_{g,o} + \int_0^x m_e dx$$
$$\dot{m}_{vapor} = n(m_{po} - m_p) \tag{25}$$

This system of equations can be regarded as an implicit system in area A. We first linearly extrapolate the area to the next node, evaluate all other variables, and then correct the area using the following set of equations:

$$\rho_g = \rho_a + \rho_w$$
$$A = \frac{\dot{m}_g}{\rho_g u_g}$$

In this way, we can iterate to get the converged value of the area. Here it was observed from the following plot of order of magnitude of relative arror in area as a function of number of iterations (Fig.(4)) that only two iterations suffice to achieve desired accuracy. Using any further iterations would be an improper use of computational resources.

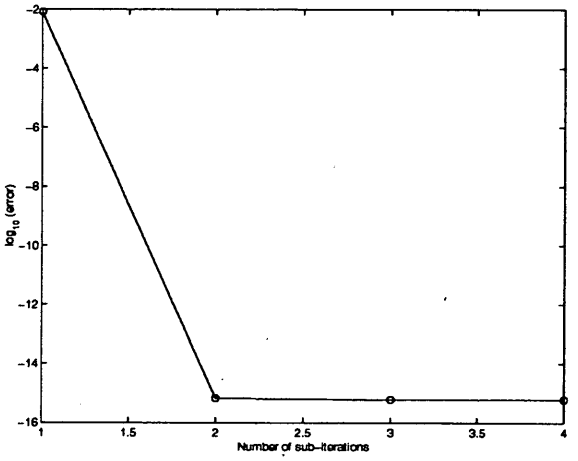

Figure 4: Variation of relative error in area with number of sub-iterations

4 Calculation of entrainment rate

In the above solution procedure it was assumed that the entrainment rate was supplied at each marching step. This section focuses on obtaining the rate of mass entrainment. Developing region and self-similar region are considered separately.

4.1 Fully developed region

Consider incompressible flow. In the self-similar region, the jet spreading rate in terms of the half-velocity thickness is given by the expression (Lele and Freund)

$$\frac{\delta_{1/2}}{D} \approx 0.095 \frac{x}{D} \tag{26}$$

The self-similar velocity profile is

$$\frac{u(\eta)}{U_c} = \left(1 + \frac{\eta^2}{4}\right)^{-2} \tag{27}$$

where $\eta = r/\delta_{sc}$ and δ_{sc} is the scaling thickness equal to $0.3884\delta_{1/2}$ (White). Momemtum flux is

$$
\begin{aligned}
M &= \rho U_c^2 \delta_{sc}^2 \int_0^\infty 2\pi\eta \tfrac{u^2}{U_c^2} d\eta \\
&= \rho U_c^2 \delta_{sc}^2 \int_0^\infty 2\pi\eta \left(1 + \tfrac{\eta^2}{4}\right)^{-4} d\eta \\
&= \rho U_c^2 \delta_{sc}^2 (4.1888)
\end{aligned}
\tag{28}
$$

Hence,

$$
U_c = \frac{1}{\delta_{sc}} \sqrt{\frac{M}{4.1888\rho}} \tag{29}
$$

An entrainment hypothesis was made which states that the turbulent fluctuating velocity that causes entrainment is proportional to the jet centerline velocity.

$$
m_e = \alpha U_c \rho_s 2\pi\delta_{sc} \tag{30}
$$

where ρ_s is the ambient density and α is the entrainment constant to be determined using the experimental data related to the jet spreading rate. This gives,

$$
\begin{aligned}
\tfrac{d\dot{m}}{dx} &= \alpha U_c \rho 2\pi\delta_{sc} \\
\Rightarrow \tfrac{d}{dx}\left\{U_c \delta_{sc}^2 \rho \int_0^\infty 2\pi\eta \left(1 + \tfrac{\eta^2}{4}\right)^{-2} d\eta\right\} &= \alpha\rho_s U_c 2\pi\delta_{sc} \\
\Rightarrow 12.5663\sqrt{\tfrac{M}{4.1888\rho}} \tfrac{d\delta_{sc}}{dx} &= \alpha\sqrt{\tfrac{M}{4.1888\rho}} 2\pi
\end{aligned}
$$

But $\delta_{sc} = 0.3884\delta_{1/2} = 0.0369x$. This gives,

$$
\alpha = 0.0738
$$

We now define the non-dimensional entrainment rate as C_2 by

$$
C_2 = \frac{D}{\rho U_c \frac{\pi}{4} D^2} \left(\frac{\rho_o}{\rho_s}\right)^{1/2} m_e \tag{31}
$$

m_o is the mass flow rate at nozzle exit and ρ_o is fluid density at nozzle exit. Here, $\rho_o = \rho_s = \rho$ since we have assumed incompressible flow.

$$
C_2 = \frac{D}{\rho U_c \pi D^2/4} \left(\frac{\rho_o}{\rho_s}\right)^{1/2} 2\pi\alpha \sqrt{\frac{M}{4.1888\rho}} \quad \rho \tag{32}
$$

But $M = \frac{\pi}{4} D^2 \rho U_c^2$. The above expression then becomes

$$
\begin{aligned}
C_2 &= \tfrac{D}{\rho U_c \pi D^2/4} \left(\tfrac{\rho_o}{\rho_s}\right)^{1/2} 2\pi\alpha D U_c \sqrt{\tfrac{\pi}{4}\tfrac{\rho}{4.1888\rho}} \quad \rho \\
&= 4\alpha \tfrac{\pi}{4.1888} \\
\Rightarrow C_2 &= 0.256
\end{aligned}
\tag{33}
$$

Ricou and Spalding (1961) state that C_2 ranges from 0.248 to 0.456. Experimental study due to Hill (1972) suggests the value 0.32 for C_2. Zaman (1998) predicts a similar value, 0.316. Since C_2 varies considerably in different studies, we adopt a representative value of 0.32.

4.2 Early development region - Compressibility effects

The developing region requires special attention as it is important from acoustics point of view. Compressibility effects in this region may be significant. They are incorporated into the present analysis. As the jet issues out of the nozzle, velocity profile is a plug profile. As the vortex sheet at the edge of the profile diffuses, the annular shear layer spreads. Spreading rate depends on the convective Mach number defined as

$$M_c = \frac{U_c}{a_e + a_{amb}} \tag{34}$$

Where U_c = Jet exit velocity
a_e = Speed of sound inside the jet at exit
a_{amb} = Speed of sound in atmosphere
Papamoschou and Murakami (2000) give an expression for spreading rate of pitot tube thickness:

$$\delta'_{pit} = 0.14(1+\sqrt{s})[0.23 + 0.77exp(-3.5M_c^2)] \tag{35}$$

where $s = \rho_{amb}/\rho_{exit}$
In the early region, sinusoidal velocity profiles were assumed in the shear layer. These profiles are:

$$\begin{aligned} u(r) = \frac{U_c}{2}\left\{1 - sin\left[\left(r - y_c - \frac{\delta}{2}\right)\frac{\pi}{\delta}\right]\right\} & y_c < r < y_c + \delta \\ = U_c \quad for \quad & r < y_c \\ = 0 \quad for \quad & r > y_c + \delta \end{aligned} \tag{36}$$

This profile gives,

$$\delta = \frac{U_c}{\left(\frac{\partial U}{\partial r}\right)_{max}} = \frac{2}{\pi}\delta_\omega$$

Temperature profile was calculated using Crocco-Busemann relation as follows. Crocco-Busemann relation states that temperature can be expressed as a function of velocity when ideal gas law is valid and Pr is nearly unity. The functional dependence can be written as

$$C_pT = -\frac{u^2}{2} + Au + B \tag{37}$$

Applying the boundary conditions:
At r = 0, u = U_c, T = T_c
At r = δ, u = 0, T = T_c
we get

$$A = [U_c^2/2 + C_{p,air}(T_c - T_\infty)]/U_c \tag{38}$$

$$B = C_{p,air}T_\infty \tag{39}$$

Using these profiles and the spreading rate data, momentum conservation can be applied to obtain thickness of the potential core. This completely describes velocity and temperature profiles. This information can then be used to compute entrainment rate using mass conservation. If M is the momentum flux at the exit of the jet then at every cross section along the jet, momentum flux remains M. This gives

$$\int_0^{y_c} \rho u^2 2\pi r dr + \int_{y_c}^{y_c+\delta} \rho u^2 2\pi r dr = M \tag{40}$$

Denoting $(r - y_c - \frac{\delta}{2})\frac{\pi}{\delta}$ by β and using the ideal gas law, we obtain:

$$\rho_c U_c^2 \pi y_c^2 + \int_{-\frac{\pi}{2}}^{\frac{\pi}{2}} \frac{P}{RT} u^2 2\pi \left(\beta\frac{\delta}{\pi} + y_c + \frac{\delta}{2}\right)\frac{\delta}{\pi} d\beta$$

$$y_c^2 + \frac{P}{R}\frac{2}{\rho_c U_c^2}\left\{\left[\int_{-\frac{\pi}{2}}^{\frac{\pi}{2}} \frac{u^2}{T} d\beta\right] y_c \frac{\delta}{\pi} + \int_{-\frac{\pi}{2}}^{\frac{\pi}{2}} \frac{u^2}{T}\left(\frac{\beta}{\pi} + \frac{1}{2}\right) d\beta \frac{\delta^2}{\pi}\right\} = \frac{D^2}{4} \tag{41}$$

Here we have used the fact that

$$M = \pi \frac{D^2}{4} \rho_c U_c^2$$

This is a quadratic in $y_c(x)$ and can be solved. Integrals appearing above are evaluated numerically and $\delta_{pit}(x)$ is supplied. δ is computed from the pitot tube thickness by using the equations (Papamoschou and Roshko, 1988):

$$\delta_{vis} \approx \frac{\delta_{pit}}{0.8} \tag{42}$$

$$\delta_\omega \approx 0.5\delta_{vis} \tag{43}$$

Having obtained velocity and temperature profiles completely, continuity equation can be used to compute entrainment rate. We have,

$$m_e = \frac{dm}{dx} = \frac{d}{dx}\int_0^{y_c+\delta} \rho u 2\pi r dr$$

Using Leibnitz rule,

$$m_e = \int_0^{y_c+\delta} \frac{\partial}{\partial x}(\rho u 2\pi r)\Big|_r dr + (\rho u 2\pi r)\Big|_{y_c+\delta} \frac{d}{dx}(y_c + \delta) - (\rho u 2\pi r)\Big|_0 \frac{d}{dx}(0)$$

Last two terms on the RHS are zero.

$$m_e = \int_{y_c}^{y_c+\delta} \frac{\partial}{\partial \beta}(\rho u 2\pi r)\Big|_r \frac{d\beta}{dx} dr + \int_0^{y_c} \frac{\partial}{\partial \beta}(\rho u 2\pi r)\Big|_r \frac{d\beta}{dx} dr$$

Second integral on the RHS is zero because both density and velocity are constant inside the potential core.

Changing variable of integration to β,

$$m_e = \int_{-\frac{\pi}{2}}^{\frac{\pi}{2}} r 2\pi \frac{\partial}{\partial \beta}(\rho u)\frac{d\beta}{dx}\frac{\delta}{\pi} d\beta \tag{43}$$

Now,

$$\frac{d}{d\beta}(\rho u) = \rho\frac{du}{d\beta} + u\frac{d\rho}{d\beta}$$
$$= \rho\frac{du}{d\beta} + u\frac{d\rho}{dT}\frac{dT}{du}\frac{du}{d\beta} \tag{44}$$

But $\rho = \frac{P}{RT}$ giving us:

$$\frac{d\rho}{dT} = -\frac{P}{RT^2}$$

Also, $T = [-\frac{u^2}{2} + Au + B]/C_p$. Hence,

$$\frac{dT}{du} = (A-u)/C_p$$
$$\Rightarrow \frac{d}{d\beta}(\rho u) = \left[\rho + u\left(-\frac{P}{RT^2}\right)\frac{(A-u)}{C_p}\right]\frac{du}{d\beta}$$

Where

$$\frac{du}{d\beta} = \frac{d}{d\beta}\left[\frac{U_c}{2}(1-sin\beta)\right] = -\frac{U_c}{2}cos\beta$$

Also,

$$\beta = \frac{\pi}{\delta}\left(r - \frac{\delta}{2} - y_c\right)$$
$$\frac{d\beta}{dx} = -\frac{\pi}{\delta^2}r\delta' + \frac{\pi}{\delta^2}y_c\delta' - \frac{\pi}{\delta}y_c' \tag{46}$$

Where dash denotes differentiation with respect to x. Now, m_e can be evaluated by numerically computing the integral in equation (43). As the shear layer grows further, it starts "feeling" the effect of its circular shape and the growth rate no longer remains constant. In the present study, the above analysis was applied upto a distance of twice the jet diameter. Beyond 13D, the constant value of C_2 corresponding to the fully developed flow is used. The middle region is interpolated using a cubic spline in the non-dimensional coordinates C_2 and x/D. Resultant variation of C_2 is plotted in figure (5).

5 Results and discussion

To generate data and highlight the effect of liquid droplets on the jet flow, we keep the geometry and exit condition of the jet fixed. Jet diameter is 29mm, jet exit Mach number is set to 1.44, stagnation temperature is 600 K. This gives jet exit velocity of 594.44 m/s and temperature at the jet exit is 424.1 K.

First we shall demonstrate certain general trends using the particle size of 26.7 microns. Figure (6) shows that the momentum coupling between the two phases causes the particle velocity to tend to follow the gas velocity. Heat coupling has a similar effect on the droplet temperature.

We set the total mass flow rate of water droplets at 10% of the jet exit mass flow rate. We then vary the droplet size to observe the droplet behaviour. From figure (7) we see that smaller particles affect the velocity history more than the larger particles do.

Some other important observations are:

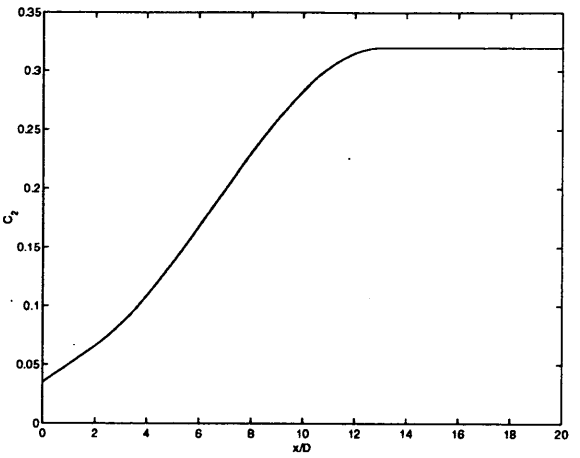

Figure 5: Cubic spline fit for non-dimensional entrainment rate

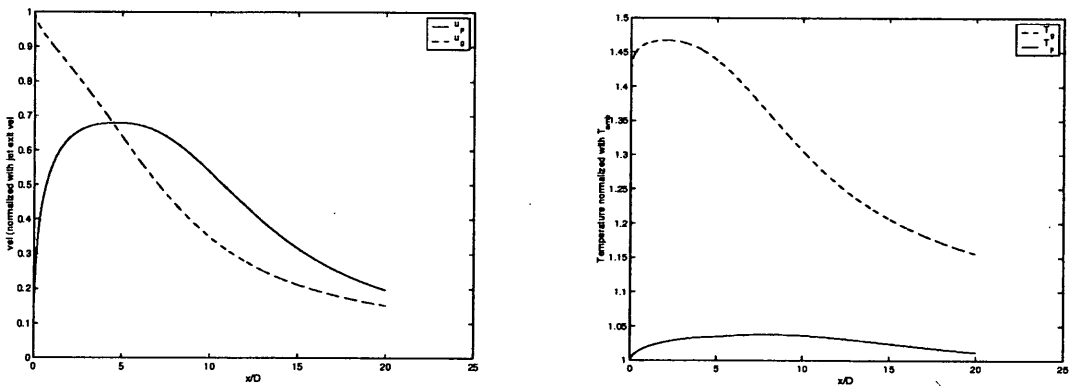

Figure 6: (a) Velocity and (b) Temperature response of a particle

- Computations were performed to evaluate the importance of surface energy change during atomization. It was found that, if every particle breaks into two, then the increase in surface energy is six orders of magnitude less than the kinetic energy of the gaseous phase. This suggests that, the mechanism of conversion of turbulent energy into surface energy is unimportant here.
- A simple modification of the formulation was done in order to accomodate different particles sizes with the corresponding number densities.
- Efficacy of Crocco-Busemann relation in conserving total energy was tested. Assuming velocity profiles and temperature profiles are same, the relative error in total energy was found to be 3% or less. After using Crocco-Busemann relation to find temperature profiles, this upper bound on the relative error in energy was reduced to 0.5%.
- Dimensional analysis suggested that the non-dimensional parameter deciding the importance of particles in mass and momentum variation was nothing but the ratio of the total mass flow of liquid droplets to the mass flow rate of gaseous phase. Also, since temperature

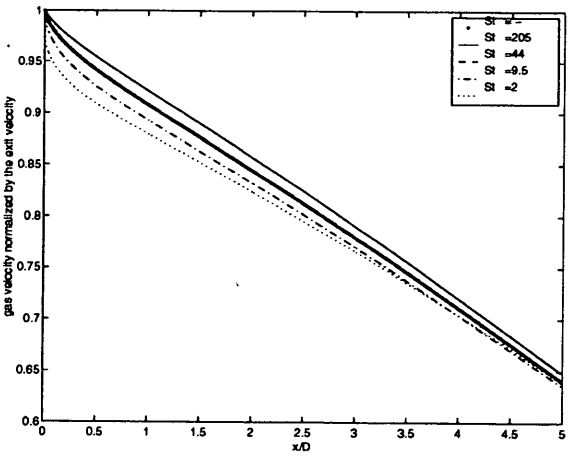

Figure 7: Effect of droplet size on main flow

variations for both the phases are approximately of the same order, the same parameter also governs energy variation. When this parameter is small, presence of the droplets may be neglected completely.

References

- Miller, R. S. and Bellan, J. (1998) "Direct numerical simulation of a confined three-dimensional gas mixing layer with one evaporating hydrocarbon-droplet-laden stream", J. Fluid Mech., Vol. 384, pp. 293-338.
- Hill, B. J. (1971) "Measurement of local entrainment rate in the initial region of axisymmetric turbulent air jets", J. Fluid Mech., Vol. 51, Part 4, pp. 773-779.
- Zaman, K. B. M. Q. (1998) "Asymptotic spreading rate of initially compressible jets - experiment and analysis", Physics of Fluids, Vol. 10, No. 10, pp. 2652-2660.
- Dimotakis, P. E., Slessor, M. and Zhuang (2000) "Turbulent shear-layer mixing: growth rate compressibility scaling", J. Fluid Mech., Vol. 414, pp. 35-45.
- Papamoschou, D. and Murakami, E. (2000) "Mixing layer characteristics of coaxial supersonic jets", 6th AIAA/CEAS Aeroacoustics Conference, June 2000, Hawaii.
- Krothapalli, A. and Washington, D. (1998) "The role of water injection on the mixing noise supersonic jet", 4th AIAA/CEAS Aeroacoustics Conference, June 1998, Toulouse, France.
- Lele, S. K. and Freund, J. B. (2001) "Computer simulation and prediction of jet noise", High Speed Jet Flows: Fundamentals and applications, Taylor Francis.
- Ricou, F. P. and Spalding, D. B. (1961) "Measurements of entrainment by axisymmetrical turbulent jets", J. Fluid Mech., Vol. 11, 21.
- Papamoschou, D. and Roshko, A. (1988) "The compressible turbulent shear layer: an experimental study", J. Fluid Mech., Vol. 197, pp. 453-477.
- Donley, H. E. (1991) "Drag force on a sphere", UMAP Journal, Module 712, Vol. 12, No. 1, Spring 1991, pp. 47-80.
  http://www.ma.iup.edu/projects/CalcDEMma/drag/drag.html